Carbon dots decorated vertical SnS_2 nanosheets for efficient photocatalytic oxygen evolution

Zhongzhou Cheng' , Fengmei Wang' , Tofik Ahmed Shifa, Kaili Liu, Yun Huang, Quanlin Liu, Chao Jiang, and Jun He'

Citation: Appl. Phys. Lett. **109**, 053905 (2016); doi: 10.1063/1.4960527
View online: http://dx.doi.org/10.1063/1.4960527
View Table of Contents: http://aip.scitation.org/toc/apl/109/5
Published by the American Institute of Physics

Carbon dots decorated vertical SnS_2 nanosheets for efficient photocatalytic oxygen evolution

Zhongzhou Cheng,[1,2,a)] Fengmei Wang,[2,3,a)] Tofik Ahmed Shifa,[2,3] Kaili Liu,[2,3] Yun Huang,[2,3] Quanlin Liu,[1] Chao Jiang,[2,3] and Jun He[2,3,b)]
[1]*School of Materials Science and Engineering, University of Science and Technology Beijing, Beijing 100083, China*
[2]*CAS Key Laboratory of Nanosystem and Hierarchical Fabrication, National Center for Nanoscience and Technology, Beijing 100190, China*
[3]*CAS Center for Excellence in Nanoscience, National Center for Nanoscience and Technology, Beijing 100190, China*

(Received 22 June 2016; accepted 25 July 2016; published online 4 August 2016)

Metal sulfides are highly desirable materials for photocatalytic water splitting because of their appropriate energy bands. However, the poor stability under light illumination in water hinders their wide applications. Here, two-dimensional SnS_2 nanosheets, along with carbon dots of the size around 10 nm, are uniformly grown on fluorine doped tin oxide glasses with a layer of nickel nanoparticles. Significantly, strong light absorption and enhanced photocurrent density are achieved after integration of SnS_2 nanosheets with carbon dots. Notably, the rate of oxygen evolution reached up to 1.1 mmol g^{-1} h^{-1} under simulated sunlight irradiation featuring a good stability. *Published by AIP Publishing.* [http://dx.doi.org/10.1063/1.4960527]

Inspired by the natural photosynthesis, researchers made effort to realize the direct conversion of solar energy into chemical fuels.[1] Photo(electro)chemical cells, mimicking the photosynthetic process within a leaf by splitting water to generate hydrogen and oxygen, have recently been focused as the potential system that would extend the natural scenario.[2,3] In this regard, the free and unlimited supply of solar energy and water is utilized in the process. The merit of its environmentally benign reactions under mild conditions without evolution of pollutants, such as carbon oxides, suggested the good application prospect. However, some factors usually inhibit the efficiency of solar water splitting. First, most of the photocatalysts (TiO_2, ZnO, etc.) only absorb the UV light, which accounts for merely 4% of the total sunlight.[4] Second, sluggish charge transfer and water oxidation kinetics in the reaction hinder the process.[5,6] Thus, further breakthroughs in the design and synthesis of an efficient photoelectrode to facilitate the charge transfer and water oxidation and eventually promote efficient light absorption hold the key to the development of water splitting.

Additionally, according to the diffusion feature of the electron-hole pairs[7] ($t = d^2/k^2D$; d is the particle size, k is a constant, D is the diffusion coefficient of electron-hole pairs), the ultrathin two-dimensional (2D) nanostructures, similar to graphene, provide more opportunities to improve the water splitting process. Such a morphology will provide high specific areas for surface photochemical reactions and enhance the efficiency of photo-generated electron-hole separation.[8] Of particular note is that the quantum confinement effects within several-atoms-thick sheets could offer a much more active site for photocatalysis under light irradiation.[9] In order to satisfy this requirement, some 2D nanomaterials, such as MoS_2,[10] CdS,[11] ZnSe,[12] and In_2O_3[13] nanosheets, were prepared through exfoliation and hydrothermal methods. Due to its nontoxic, chemically stable nature in neutral aqueous solution and low cost characteristics, hexagonal tin disulfide (SnS_2), possessing the visible-light band gap of 2.2–2.4 eV, attracts the interests of the researchers.[14–17] It has a CdI_2-type structure consisting of S-Sn-S triple layers that are connected together by weak van der Waals forces. Despite these appealing features, there are only few reports hitherto about uniform SnS_2 nanosheet (FS) arrays for photocatalytic water splitting specifically meant for producing oxygen gas. This can be associated with the difficulty of synthesizing such nanosheets in a large scale, without any aggregation, that would effectively handle the catalysis of sluggish and four electron consuming steps in oxygen evolution reaction.

Herein, carbon dot (CD) decorated vertical ultrathin SnS_2 nanosheet arrays were grown uniformly on fluorine doped tin oxide (FTO) glass with a 10 nm layer of nickel nanoparticles (Nps) via the solvothermal method. Interestingly, strong light absorption and enhanced photocurrent density are achieved after the integration of CDs, SnS_2 nanosheets, and Ni Nps on the FTO. This photoelectrode exhibits a high photocatalytic oxygen evolution activity of 1.1 mmol g^{-1} h^{-1} under simulated sunlight irradiation in the presence of aqueous KIO_3 solution as a sacrificial agent. Moreover, our integrated photocatalyst demonstrates a very good stability for consistently catalyzing the obviously known sluggish steps of oxygen evolution reaction.[18,19]

The FTO was thoroughly cleaned with acetone, ethanol, and deionized water in sequence, and then put into 40 ml ethanolic solution containing 20 mM of $SnCl_4$ and 60 mM of CH_3CSNH_2. The content was then sealed in an autoclave and treated at 70 °C for 6 h. Finally, the FTO was taken out, washed with deionized water, and dried at room temperature to obtain vertically oriented SnS_2 nanosheets (FS).[20] For

a)Z. Cheng and F. Wang contributed equally to this work.
b)Author to whom correspondence should be addressed. Electronic mail: hej@nanoctr.cn

incorporating Ni NPs, we followed the same procedure as FS except depositing 10 nm of Ni layer onto the surface of FTO via the thermal evaporation method (FNS). The as obtained nanosheet was immersed in 0.5 mol l^{-1} glucose aqueous ethanolic (ethanol to water volume ratio of 1: 1) solution and kept there for 4 h to reach the surface saturation level of adsorption equilibrium. Next, it was taken out and dried at room temperature before being placed in the center of Ar saturated tube furnace. The furnace temperature was then slowly raised to 500 °C keeping a vacuum environment for 1.5 h.[21,22] After cooling the furnace, we obtained carbon dot decorated SnS_2 nanosheets (FSC). And the "FNSC" means the "carbon dot decorated SnS_2 nanosheets" on the FTO onto which 10 nm of Ni layer was deposited.

Scanning electron microscopy (SEM) images were obtained from a Hitachi S4800 field-emission scanning electron microanalyzer with an accelerating voltage of 10 kV, and the corresponding energy-dispersive X-ray spectroscopy (EDX) spectrum was obtained under an accelerating voltage of 20 kV. High-resolution transmission electron microscopy (HRTEM) images and selected area electron diffraction (SAED) patterns were obtained from a Tecnai G2 F20 with a beam energy of 200 keV. UV-vis-NIR spectra were recorded using a Lambda 950 spectrophotometer equipped with an integrating sphere. X-ray diffraction patterns (XRD) were obtained from a D/MAX-TTRIII (CBO) system using a Cu-Kα radiation ($\lambda = 1.5418$ Å). Raman spectra were measured at room temperature on an InVia RENISHAW system at the excitation line of 532 nm. The Raman band of Si at 520 cm^{-1} was used as a reference to calibrate the spectrometer.

Photocurrent measurements were conducted in a typical three electrode electrochemical system (CHI-660D), under visible light illumination (Xenon lamp, 100 mW cm^{-2}, $\lambda > 420$ nm) with zero bias versus saturated calomel electrode (SCE). Photo-catalytic water splitting experiments were conducted in a 500 ml cylinder quartz reactor under photo irradiation conditions that was coupled with a gas chromatograph (GC-14C, Shimadzu, Japan, TCD, nitrogen as a carrier gas and 5 Å molecular sieve column) at ambient temperature. A 300 W xenon lamp with a simulated sunlight filter (light intensity was 300 mW cm^{-2}) used as a light source. In a typical O_2 evolution experiment, the prepared photocatalyst was placed at the bottom of reactor containing 100 ml deionized water containing 1.07 g of KIO_3 powder. Before irradiation, the system was vacuumed for about 30 min to remove the air inside and to ensure that the system was under the anaerobic condition. A certain amount of generated gas was intermittently sampled through septum and analyzed by gas chromatography. A base-line was recorded for each test before exposure to the xenon lamp.

In order to enhance the adhesion strength between the nanosheets and substrate, a layer of nickel nanoparticles (10 nm) were thermally evaporated on the surface of FTO before the growth. Fig. 1(a) shows the scanning electron microscopy (SEM) images of the as-prepared ultrathin vertical SnS_2 nanosheets (FNS), which seem like standing walls with the larger size of 500 nm (the inset of Fig. 1(a)). As can be seen in Fig. 1(b), densely populated carbon dots (CDs) with the diameter of around 10 nm were formed evenly on SnS_2 nanosheets grown on the FTO substrate. The CDs also increase the

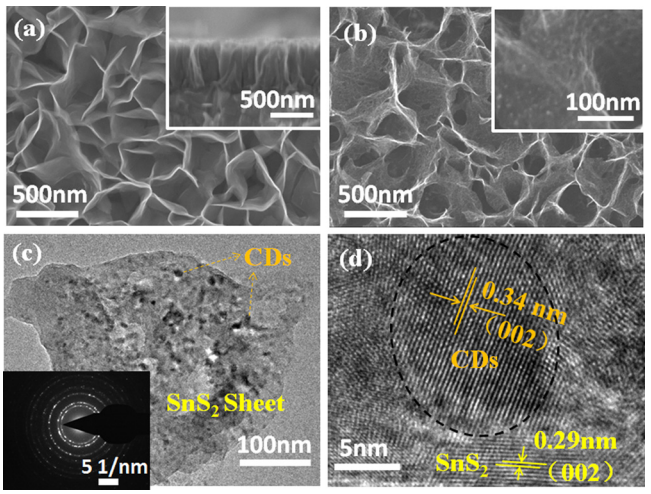

FIG. 1. (a) SEM images of the SnS_2 nanosheet on FTO substrate; Inset: a side-view. (b) SEM images of Carbon Dots decorated SnS_2 nanosheets; Inset: an enlarged view of Carbon Dots. (c) Typical TEM image of Carbon Dots (CDs) on the SnS_2 nanosheet; Inset: corresponding SAED image. (d) HRTEM image of CDs and SnS_2 nanosheets, showing the distinguishable lattice spacing for C and SnS_2.

conductivity of the photoelectrodes, which leads to higher ion exchange rate and faster electron transport. Fig. 1(c) depicts the transmission electron microscopic (TEM) image of the sample. The CDs with the size of about 10 nm are abundantly distributed on the top surface of the SnS_2 nanosheet, which is consistent with the SEM observation. The inset of Fig. 1(c) shows the selected area electron diffraction (SAED) pattern with two noticeable rings, suggesting the polycrystalline SnS_2 and CDs. The inner ring ($r = 2.93\ nm^{-1}$, $d = 1/r = 0.34$ nm) and outer ring ($R = 3.41\ nm^{-1}$, $d = 0.29$ nm) are ascribed to CDs (plane (002), PDF#34-0046) and SnS_2 nanosheets (plane (002), PDF#75-0367), respectively, which agree well with the reported literature.[23] We found distinguishable characteristic features of SnS_2 and the CDs from the HRTEM image (Fig. 1(d)) wherein the lattice spacings of 0.34 nm and 0.29 nm were evidenced for CDs (plane (002)) and SnS_2 (plane (002)), respectively.[23] Moreover, the CDs are embedded into the polycrystalline SnS_2 nanosheets, further revealing the well-integrated feature of our material that is greatly expected to contribute to a faster transport of the photo-generated charge carriers.

Energy Dispersive X-Ray Spectroscopy (EDX) was used to determine the elemental composition in the as-synthesized materials (Fig. 2(a)). It is apparent that the atomic ratio of Sn and S is about 1: 2. The Raman spectrum shown in Fig. 2(b) suggests a strong peak at 313 cm^{-1}, indicating the existence of SnS_2.[24] And the peak 1435 cm^{-1} can be attributed to amorphous Carbon.[25] XRD patterns of FTO and FNSC samples are displayed in Fig. 2(c). Apart from the XRD pattern of FTO, the peaks at 28.5° and 50.4° can be assigned to SnS_2 (PDF#75-0367), corresponding to the planes (100) and (110), respectively. And the peaks at 26.5° and 54.7° are due to the (002) and (004) planes of the Carbon (PDF#34-0046). UV-visible-infrared diffusive reflectance absorption spectroscopy (Abs) was used to further investigate the as-prepared nanomaterials (Fig. 2(d)). Compared with the absorption spectra of the FTO-SnS_2 (FS), samples such as FTO-C (FC), FTO-SnS_2-C (FSC), and FTO-

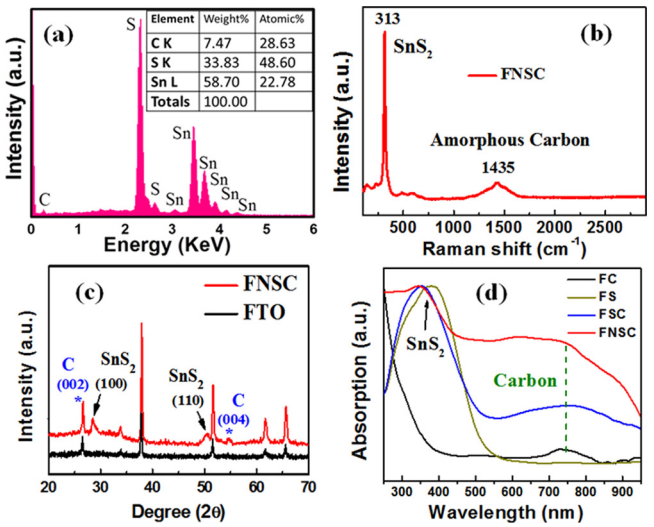

FIG. 2. (a) EDX spectrum of the sample; Inset: elemental composition profile. (b) Raman spectrum of the FNSC sample. (c) XRD patterns of the FTO and FNSC sample. (d) UV/vis/NIR diffusive reflectance absorption spectra of FC, FS, FSC, and FNSC samples.

Ni-SnS_2-C (FNSC) demonstrate a strong absorption around 730 nm, which indicates the increased light absorption after the CD decoration. Owing to the quantum effects, the CDs exhibit band gaps different from the bulk[26] and show a strong light-absorption under visible light irradiation. Due to various sizes of the CDs, the electrodes decorated with CDs possess a broadening absorption peak, thus improving the light absorption.

To investigate the photocurrent properties of the as-prepared electrodes, the photoelectrochemical (PEC) measurements were conducted in a three-electrode setup containing 0.5 mol l^{-1} Na_2SO_4 solution without any bias. And the visible light ($\lambda > 420$ nm) with the power density of 100 mW cm^{-2} was utilized as the illumination source. Fig. 3(a) demonstrates typical time-dependent current change curves of the different electrodes. As a comparison, the pure FTO (F), FTO-SnS_2 (FS), and FTO-Ni-SnS_2 (FNS) electrodes were also measured. The negligible photo-response of the FTO suggested that the observed photocurrent is only due to the catalysts grown on the surface. Notably, the photocurrent density of the FNSC electrode rapidly increased to 38.6, which is about twice larger than that of FNS electrode (19.8 μA cm^{-2}), under light illumination. From the UV-vis spectra in Fig. 2(b), it appears conclusive that the CDs on the surface of the nanosheets can enhance the absorption of light which in turn densify light-induced electrons. It is also obvious that the introduction of the Ni layer can improve the conductivity of the electrode and facilitate the separation of the photo-generated electro-hole pairs, resulting in a higher photocurrent density (19.8 μA cm^{-2}) than that (16.6 μA cm^{-2}) of FS electrode. Additionally, Fig. 3(b) shows the electrochemical impedance spectroscopy (EIS) spectrum of the various electrodes (FS, FNS, and FNSC) at zero bias. Compared with FS and FNS, lower impedance is recorded for FNS, meaning the conductivity was enhanced with the deposition of the Ni layer. The smallest circle of the FNSC electrode indicates that the incorporation of CDs enhanced electron-hole pair separation.

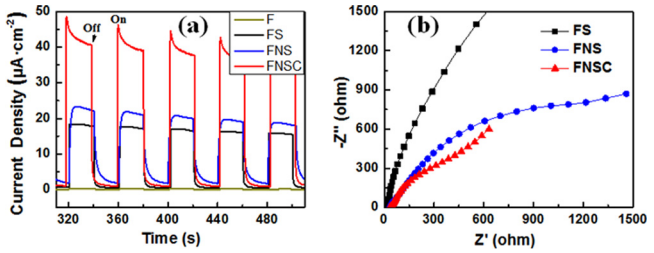

FIG. 3. (a) Photocurrent responses of the different sample electrodes to on/off cycles, under illumination of visible light (Xenon lamp, 100 mW cm^{-2}, $\lambda > 420$ nm) and zero bias versus saturated calomel electrode (SCE). (b) EIS plots of the different sample electrodes, with zero bias.

The photocatalytic activities of the various electrodes were further evaluated for the generation of oxygen under simulated solar-light at room temperature. Typically, a piece of FTO glasses (2×4 cm^2) covered with the nanomaterial (about 14 mg, all the sample would be accurately weighed before the experiment) was place in the quartz electrolytic cell containing 100 ml deionized water wherein 1.07 g of KIO_3 powder (50 mM) was dissolved in it. The KIO_3 was utilized as a sacrificial agent to consume the light-generated electrons. A 300 W xenon lamp equipped with a simulated sunlight (AM 1.5 G) filter was used as a light source. At given irradiation time intervals (1 h), the generated oxygen gas was collected and detected with the gas chromatography (GC). The results are shown in Fig. 4(a). The FS electrode demonstrates poor photocatalysis and stability under light illumination within 3 h. After 3 h, its ability of oxygen generation was further decreased owing to the oxidation of the exposed SnS_2 nanosheets.[27] The incorporation of Ni nanoparticles into the sample FNS, to a certain extent, improves the ability of oxygen evolution to 0.7 mmol g^{-1} h^{-1}. However, the poor stability of these electrodes impedes their practical application. Importantly, the sample of FNSC exhibits a high efficiency within 3 h under light irradiation. And the rate of the oxygen evolution based on the FNSC electrode is about 1.1 mmol g^{-1} h^{-1}, which is comparable to some reported

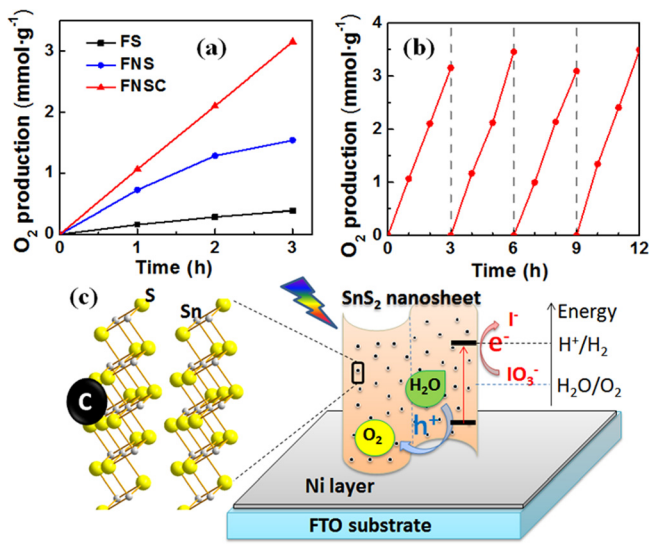

FIG. 4. (a) Plots of the oxygen evolution rate through direct photo-catalysis for FS, FNS, and FNSC samples. (b) Cycling measurements of Oxygen gas generation based on the FNSC sample for 12 h under simulated solar light. For each cycle O_2 inside was removed after every 3 h. (c) A schematic diagram of water splitting by the FNSC sample.

works.[18,20,28,29] This can be attributed to the facts that, on the one hand, the CDs covering the surface of SnS_2 nanosheets protect the catalyst from being oxidized;[30,31] and on the other hand, the CDs by themselves enhanced light absorption and hence photocurrent to provide a further boost for O_2 evolution. To evaluate the stability of the FNSC samples under simulated solar light, testing cycles are displayed in Fig. 4(b). Through four continuous testing cycles during 12 h, FNSC did not exhibit obvious degradation, indicating its high O_2 production capability. During the stability measurement, of each cycle O_2 found inside the system was removed after every 3 h. Finally, a schematic diagram of water splitting by the FNSC sample is presented in Fig. 4(c) depicting the fact that the ultrathin SnS_2 nanosheets covered with CDs were grown on the FTO substrate with a 10 nm layer of nickel nanoparticles. Under the light illumination, the excited electrons were consumed by the sacrificial agent to reduce the IO_3^- to I^-, while the generated holes are utilized to oxidize the H_2O molecule to O_2. Significantly, the unique photo-induced electron transfer and photo adsorption properties in this system[32] promote the oxygen evolution on the surface. The nanostructure designed in this study broadens the practical application of the earth-abundant and low-cost photocatalyst for splitting water.

In summary, vertical ultrathin SnS_2 nanosheets were synthesized on FTO substrates using a hydrothermal method. After introducing a layer of Ni nanoparticles, the conductivity of the system was enhanced. Notably, the CDs on the surface not only protect the SnS_2 nanosheets from being oxidized under light but also increase the light absorption to generate much more electron-hole pairs. The FNSC electrode shows a high rate of oxygen evolution under simulated solar light. The long-time test cycles further confirm the potential utilization of this nanostructure in a large scale. We believe that our research will provide an easy method to resolve the problem for the stability in water splitting reaction of sulfide based catalysts.

This work was supported by the National Natural Science Foundation of China (Nos. 21373065, 61474033 and 61574050), Strategic Priority Research Program of the Chinese Academy of Sciences (Grant No. XDA09040201), 973 Program of the Ministry of Science and Technology of China (No. 2012CB934103), and CAS Key Laboratory of Nanosystem and Hierarchical Fabrication. The authors also gratefully acknowledge the support of Youth Innovation Promotion Association CAS.

[1]J. Michl, Nat. Chem. **3**, 268 (2011).
[2]B. Matthews, J. Jansonius, P. Colman, B. Schoenborn, and D. Dupourque, Nat. New Bio. **238**, 37–41 (1972).
[3]Z. Yi, J. Ye, N. Kikugawa, T. Kako, S. Ouyang, H. S. Williams, H. Yang, J. Cao, W. Luo, and Z. Li, Nat. Mater. **9**, 559 (2010).
[4]H. M. Tabaei, M. Kazemeini, and M. Fattahi, Sci. Iran. **19**, 1626 (2012).
[5]J. Zhang, J. Yu, Y. Zhang, Q. Li, and J. R. Gong, Nano Lett. **11**, 4774 (2011).
[6]S. Hoang, S. Guo, N. T. Hahn, A. J. Bard, and C. B. Mullins, Nano Lett. **12**, 26 (2012).
[7]Y. Sun, H. Cheng, S. Gao, Z. Sun, Q. Liu, Q. Liu, F. Lei, T. Yao, J. He, and S. Wei, Angew. Chem. Int. Ed. **51**, 8727 (2012).
[8]Y. Sun, Y. Xie, C. Wu, S. Zhang, and S. Jiang, Nano Res. **3**, 620 (2010).
[9]Y. Zhao, Y. Xie, X. Zhu, S. Yan, and S. Wang, Chem.-Eur. J. **14**, 1601 (2008).
[10]D. Hennig and C. Mulhern, Eur. Phy. J. B **85**, 1 (2012).
[11]Y. Xu, W. Zhao, R. Xu, Y. Shi, and B. Zhang, Chem. Commun. **49**, 9803 (2013).
[12]Y. Sun, Z. Sun, S. Gao, H. Cheng, Q. Liu, J. Piao, T. Yao, C. Wu, S. Hu, and S. Wei, Nat. Commun. **3**, 1057 (2012).
[13]F. Lei, Y. Sun, K. Liu, S. Gao, L. Liang, B. Pan, and Y. Xie, J. Am. Chem. Soc. **136**, 6826 (2014).
[14]H. Geng, Y. Su, H. Wei, M. Xu, L. Wei, Z. Yang, and Y. Zhang, Mater. Lett. **111**, 204 (2013).
[15]J. Chao, Z. Xie, X. Duan, Y. Dong, Z. Wang, J. Xu, B. Liang, B. Shan, J. Ye, and D. Chen, CrystEngComm **14**, 3163 (2012).
[16]R. Wei, J. Hu, T. Zhou, X. Zhou, J. Liu, and J. Li, Acta Mater. **66**, 163 (2014).
[17]P. Chen, Y. Su, H. Liu, and Y. Wang, ACS Appl. Mater. Interface **5**, 12073 (2013).
[18]F. Wang, Y. Wang, X. Zhan, M. Safdar, J. Gong, and J. He, CrystEngComm **16**, 1389 (2014).
[19]J. Li and N. Wu, Catal. Sci. Technol. **5**, 1360 (2015).
[20]D. V. Shinde, S. A. Patil, K. Cho, D. Y. Ahn, N. K. Shrestha, R. S. Mane, J. K. Lee, and S. H. Han, Adv. Funct. Mater. **25**, 5739 (2015).
[21]W. H. Hung, S. N. Lai, and A. Y. Lo, ACS Appl. Mater. Interface **7**, 8412 (2015).
[22]J. Roggenbuck, G. R. Koch, and M. Tiemann, Chem. Mater. **18**, 4151 (2006).
[23]A. Yella, E. Mugnaioli, H. A. Therese, M. Panthoüfer, U. Kolb, and W. Tremel, Chem. Mater. **21**(12), 2474 (2009).
[24]Y. Huang, H. X. Deng, K. Xu, Z. Wang, Q. Wang, F. M. Wang, F. Wang, X. Y. Zhan, S. S. Li, and J. W. Luo, Nanoscale **7**, 14093 (2015).
[25]M. S. Dresselhaus, A. Jorio, M. Hofmann, G. Dresselhaus, and R. Saito, Nano Lett. **10**, 751 (2010).
[26]H. Ding, S. B. Yu, J. S. Wei, and H. M. Xiong, ACS Nano **10**, 484–491 (2016).
[27]J. Yu, C. Y. Xu, F. X. Ma, S. P. Hu, Y. W. Zhang, and L. Zhen, ACS Appl. Mater. Interface **6**, 22370 (2014).
[28]S. S. K. Ma, K. Maeda, T. Hisatomi, M. Tabata, A. Kudo, and K. Domen, Chem.–Eur. J. **19**, 7480 (2013).
[29]Y. Dou, S. Zhang, T. Pan, S. Xu, A. Zhou, M. Pu, H. Yan, J. Han, M. Wei, and D. G. Evans, Adv. Funct. Mater. **25**, 2243 (2015).
[30]J. Liu, Y. Liu, N. Liu, Y. Han, X. Zhang, H. Huang, Y. Lifshitz, S. T. Lee, J. Zhong, and Z. Kang, Science **347**, 970 (2015).
[31]P. Zhang, T. Wang, X. Chang, L. Zhang, and J. Gong, Angew. Chem. Int. Ed. **55**, 5851 (2016).
[32]H. Li, Z. Kang, Y. Liu, and S.-T. Lee, J. Mater. Chem.**22**, 24230 (2012).